

Imitation Learning from Observation through Optimal Transport

Wei-Di Chang¹, Scott Fujimoto¹, David Meger¹, and Gregory Dudek¹

Abstract—Imitation Learning from Observation (ILfO) is a setting in which a learner tries to imitate the behavior of an expert, using only observational data and without the direct guidance of demonstrated actions. In this paper, we re-examine the use of optimal transport for IL, in which a reward is generated based on the Wasserstein distance between the state trajectories of the learner and expert. We show that existing methods can be simplified to generate a reward function without requiring learned models or adversarial learning. Unlike many other state-of-the-art methods, our approach can be integrated with any RL algorithm, and is amenable to ILfO. We demonstrate the effectiveness of this simple approach on a variety of continuous control tasks and find that it surpasses the state of the art in the ILfO setting, achieving expert-level performance across a range of evaluation domains even when observing only a single expert trajectory *without* actions.

I. INTRODUCTION

Imitation Learning (IL) is a widely used and effective tool for teaching robots complex behaviors. Although Reinforcement Learning (RL) has demonstrated success in learning motor skills from scratch in real-world systems [1], [2], Imitation Learning (IL) remains a proven and practical way to learn behaviors from demonstrations, without the need for a hand-tuned and engineered reward signal required for RL. However, acquiring access to expert actions can be highly impractical. For example, robotic systems which are too challenging to smoothly teleoperate, or in applications where the action spaces of the demonstrator and the imitator do not match, such as in Sim-to-Real problems [3].

Imitation Learning from Observation (ILfO) eliminates the need for demonstrated actions by learning behaviors from sequences of expert states, instead of requiring both expert states and actions. While IL algorithms often rely on teleoperation to demonstrate behavior, ILfO algorithms learn from observational data alone, similar to how humans learn new skills by watching others. ILfO algorithms can reduce the cost of data collection of robot behavior, making them instrumental for deploying IL in complex real-world robotics systems, and open the door to more complex downstream tasks, such as learning from visual demonstrations.

Moving to the observation-only space however, introduces new challenges. While IL algorithms can learn by matching demonstrated actions, ILfO algorithms require more exploration to succeed [4], as they can only imitate the state trajectories of an expert indirectly, through observed outcomes of an unknown state transition function, and without the direct guidance of demonstrated actions. This emphasis on exploration creates a further challenge in that the states visited by

the learner are more likely to be distant or non-overlapping with those of the expert. This is problematic for imitation via distribution matching [5], [6], [7], as the widely used KL divergence is ill-defined for non-overlapping distributions and may provide a poor signal when the behavior of the learner is distinct from the expert. While IL methods can circumvent this problem by accelerating early learning with behavior cloning, ILfO methods must deal with randomly initialized policies, which are unlikely to behave similarly to an expert demonstrator.

The field of optimal transport has garnered much attention in recent years, with theoretical and computational developments allowing its use for evaluating distances between distributions defined on high-dimensional metric spaces [8], [9]. The Wasserstein distance, in particular, can compare non-overlapping distributions, as well as quantify the spatial shift between the supports of the distributions. These properties make it a natural alternative to KL divergence-based objectives used by existing methods. Moreover, the Wasserstein distance can be computed without requiring separate models or learned components. This makes the Wasserstein distance more computationally efficient and conceptually simpler than other methods that rely on incremental adversarial signals learned via online interaction [5], [10], [11].

Prior work based on the Wasserstein distance for IL or ILfO rely on numerous techniques, such as adversarial or learned components, or designed for sample-inefficient on-policy RL algorithms. However, we find that we can significantly simplify an existing approach, Sinkhorn Imitation Learning (SIL) [11], removing adversarial components which rely on on-policy learning. The resulting approach, Observational Off-Policy Sinkhorn (OOPS) generates a reward function for *any* RL algorithm, which minimizes the Wasserstein distance between expert and learner state trajectories. We benchmark our approach against existing methods proposed to optimize the Wasserstein distance [11], [12], as well as current state-of-the-art ILfO algorithms [6], [13] on a variety of continuous control tasks. Our approach outperforms state-of-the-art methods for ILfO, achieving near-expert performance in every evaluated task with only a single trajectory, without observing any actions. To facilitate reproducibility, all of our code is open-sourced¹.

II. BACKGROUND

Setting. Our task is formulated by an episodic finite-horizon MDP $(\mathcal{S}, \mathcal{A}, \mathcal{P}, r, p_0, T)$, with state space \mathcal{S} , action space \mathcal{A} , transition dynamics $\mathcal{P} : \mathcal{S} \times \mathcal{A} \times \mathcal{S} \rightarrow [0, 1]$,

¹Center for Intelligent Machines, McGill University, Montréal, Canada. {wchang, sfujim, dmeger, dudek}@cim.mcgill.ca.

¹<https://github.com/weidi-chang/OOPS>

reward function $r : \mathcal{S} \times \mathcal{A} \rightarrow \mathbb{R}$, initial state distribution $p_0 : \mathcal{S} \rightarrow [0, 1]$, and T the horizon. While the overarching objective is to maximize reward, in the Imitation Learning from Observation (ILfO) setting, the agent never observes the true reward. Instead, ILfO algorithms must use sequences of states (trajectories τ), generated by an unknown expert, to infer a reward signal, or objective. We therefore only assume access to a dataset D_E of N state-only trajectories, $D_E = \{\tau_0, \tau_1, \dots, \tau_{N-1}\}$.

Optimal Transport. Optimal Transport (OT) seeks to compute a matching between the two measures (source and target) while minimizing the transport cost [14]. In our work, we aim to minimize the distance between the distribution of trajectories defined by the learner and the expert.

Writing out trajectories in terms of their transitions $\tau = \{(s_0, s_1), (s_1, s_2), \dots, (s_{T-1}, s_T)\}$, and viewing each transition as a datapoint, forms a discrete measure α over the state transition space $\mathcal{S} \times \mathcal{S}$, with weights \mathbf{a} and locations $(s_i, s_{i+1})_E \in \mathcal{S} \times \mathcal{S}$ for the expert: $\alpha = \sum_{i=0}^{T-1} a_i \sigma_{(s_i, s_{i+1})_E}$ where $\sigma_{(s_i, s_{i+1})}$ is the Dirac delta function at position (s_i, s_{i+1}) . Similarly for the learner, with weights \mathbf{b} and locations $(s_i, s_{i+1})_\pi$ for the learner, the trajectory rollout forms the measure $\beta = \sum_{i=0}^{T-1} b_i \sigma_{(s_i, s_{i+1})_\pi}$ [15]. In each trajectory we consider each timestep as being equally important, and as such restrict the weight vectors \mathbf{a} and \mathbf{b} to the uniform weight vectors: $\sum_{i=0}^{T-1} a_i = 1, a_i = \frac{1}{T} \forall 0 < i < T$, and $\sum_{i=0}^{T-1} b_i = 1, b_i = \frac{1}{T} \forall 0 < i < T$.

While the Monge formulation of OT enforces a one-to-one matching between measures, the Kantorovich formulation relaxes the OT problem by allowing each source point to split mass: the mass at any source point may be distributed across several locations [14], [15]. This provides the Wasserstein distance (or Kantorovich metric) over a distance metric d :

$$W_p(\alpha, \beta) := \left(\min_P \left(\sum_i^T \sum_j^T d(\alpha_i, \beta_j)^p P_{i,j} \right) \right)^{\frac{1}{p}}, \quad (1)$$

which uses a coupling matrix $P \in \mathbb{R}_+^{n \times m}$, where $P_{i,j}$ is the mass flowing from bin i to bin j :

$$P \in \mathbb{R}^{n \times m} \text{ such that } \sum_j P_{i,j} = \mathbf{a} \text{ and } \sum_i P_{i,j} = \mathbf{b}. \quad (2)$$

The optimal coupling P between α and β gives us the minimal cost transport plan between the measures defined by the trajectories τ_π and τ_E .

Sinkhorn distance. The Sinkhorn distance W_{Sk} is an entropy regularized version of the Wasserstein distance [8], for W_1 , with $p = 1$ this equals:

$$W_{\text{Sk}}(\tau_\pi, \tau_E) := \min_{\tilde{P}} \sum_{i=0}^T \sum_{j=0}^T d(\alpha_i, \beta_j) \tilde{P}_{i,j} - \lambda \mathcal{H}(\tilde{P}),$$

where the entropy term $\mathcal{H}(\tilde{P}) := \sum_{i=0}^T \sum_{j=0}^T \tilde{P}_{i,j} \log \tilde{P}_{i,j}$. For any given value of $\lambda > 0$, the optimal coupling matrix \tilde{P} for W_{Sk} can be computed efficiently using the iterative Sinkhorn algorithm [16]. At the cost of convergence speed, as λ approaches 0, the Wasserstein distance is recovered, while

increasing its value blurs out the transport matrix and spreads the mass between the two measures. This approximation is useful as it provides a computationally efficient method for estimating the optimal coupling matrix for the Wasserstein distance $\tilde{P} \approx P$ for small λ , where W_{Sk} upper bounds W_1 .

III. RELATED WORK

Imitation Learning. Learning from Demonstrations (LfD) approaches can be generally classified into two types of approaches: IL methods which learn directly from expert data and Inverse Reinforcement Learning (IRL) methods [17] which first infer a reward function to subsequently optimize with RL. GAIL [5] and related methods [10], [18] leverage adversarial training. Such methods have been shown to optimize a distribution matching objective between the state-action distribution of the learner and the expert, in terms of various probability divergence metrics [5], [6], [19], [7]. Each divergence objective leads to distinct imitative behavior (zero-forcing or mean-seeking or both) which can be exploited in different scenarios [20]. In contrast, our approach minimizes a Wasserstein distance-based objective, better suited for the ILfO context we operate in.

Imitation Learning from Observations. Due to the challenging nature of ILfO, many methods rely on learning a model, via an inverse dynamics model used to infer the missing actions of the expert [21], use objectives based on the transition dynamics of the expert [22], [23], or simply model the entire MDP [4]. Adversarial methods have also been adapted from the IL context [24], [25]. Another common theme is f -divergence minimization, [7] derive an approach based on the analytical gradients of f -divergences and show that different variants (FKL, RKL, JS) can be achieved through their framework. OPOLO [13], leverages off-policy learning on top of an inverse dynamics model and adversarial training. As opposed to existing methods, our approach leverages the Wasserstein distance to compute a non-adversarial and model-free reward for ILfO.

Optimal Transport for Imitation Learning. Minimization of the Wasserstein distance for IL has been previously considered in [26], [27] through Wasserstein Generative Adversarial Network (WGAN)-inspired approaches [28]. In an adversarial policy learning set up similarly to GAIL [5] and by restricting the discriminator to be a 1-Lipschitz function, these approaches can minimize the W_1 distance between the policy and the reference trajectory data distribution. However these methods suffer from the drawbacks of adversarial frameworks, which are hard to optimize and tune [29], and have been shown to be poor estimators of W_1 [30].

More recent works [11], [12], [31] make use of Wasserstein distance solvers, or related approximations, for IL. Our approach is closely based on Sinkhorn Imitation Learning (SIL) [11], which uses the Sinkhorn distance [8] to compute an entropy regularized Wasserstein distance between the state-action occupancy of the learner and expert. However, rather than use an upper bound defined by off-policy samples, they use on-policy RL [32] to optimize the cosine distance over the representation space of an adversarial discriminator

trained alongside the imitation agent. In our work, we found that we are able to vastly improve sample-efficiency by using an off-policy agent instead, and are able to consider a simpler objective without adversarial or learned representations, an aspect previously thought required for good performance. Another related approach, PWIL [12], uses a greedy formulation of the Wasserstein distance, and matches the current state-action pair (s, a) to its closest counterpart in the expert demonstration dataset at every step of the rollout. In our experimental analysis (Figure 3), we show that our approximation via the Sinkhorn distance creates a tighter upper bound of the true Wasserstein distance, and that it is a crucial aspect for consistent performance. Furthermore, we focus on ILfO, giving new insights of the capabilities of OT in this context, and show that our approach matches or outperforms existing state of the art methods.

IV. WASSERSTEIN IMITATION LEARNING FROM OBSERVATIONAL DEMONSTRATIONS

In this section, we introduce our approach for minimizing the Wasserstein distance between expert trajectories and learner rollouts. To do so, we derive a reward function based on the distance between state transitions in pairs of trajectories.

Deriving a reward from the Wasserstein distance. With the absence of a true reward signal, the ILfO setting can be framed as a divergence-minimization problem, where the objective is to match the trajectory distributions of the learner and the expert. In our case, we choose the Wasserstein distance as a metric for this task. Unlike the widely used KL divergence, the Wasserstein distance is defined for distributions with non-overlapping support, making it amenable to scenarios where the behavior of the learner and the expert may be particularly distinct. We can define our ILfO task as minimizing the Wasserstein distance W_1 between trajectories τ_π sampled from the learner policy π and example trajectories τ_E provided by an expert E :

$$\min_{\pi} \mathbb{E}_{\tau_\pi, \tau_E} [W_1(\tau_\pi, \tau_E)] = \min_{\pi} \mathbb{E}_{\tau_\pi, \tau_E} \left[\min_P \left(\sum_{i=0}^T \sum_{j=0}^T d((s_i, s_{i+1})_\pi, (s_j, s_{j+1})_E) P_{i,j} \right) \right]. \quad (3)$$

As the Wasserstein distance between a pair of trajectories can be defined as a sum over each of the transitions in each trajectory, for a given coupling matrix P , we can define a reward function

$$\tilde{r}_t(s_t, s_{t+1} | \tau_\pi, \tau_E, P) := - \sum_{j=0}^T d((s_t, s_{t+1})_\pi, (s_j, s_{j+1})_E) P_{t,j}, \quad (4)$$

such that summing the reward \tilde{r}_t over a given learner trajectory τ_π is exactly equal to the Wasserstein distance

$$W_1(\tau_\pi, \tau_E) = \min_P \left(- \sum_{i=0}^T \tilde{r}_t(s_t, s_{t+1} | \tau_\pi, \tau_E, P) \right). \quad (5)$$

Algorithm 1 OOPS

- 1: **Input:** Dataset of expert demonstrations D_E .
 - 2: **for** episodes $n = 1, \dots, N$ **do**
 - 3: Collect a trajectory from the environment.
 - 4: Compute the coupling matrix P using the Sinkhorn algorithm [16].
 - 5: Compute the reward \tilde{r} with D_E and P (Equation (4)).
 - 6: Train learner with a RL algorithm, and the collected trajectories and reward \tilde{r} .
-

This naturally suggests an objective that involves the summation of rewards \tilde{r}_t over learner trajectories

$$J(\pi | E, P) := \mathbb{E}_{\pi, E} \left[\sum_{t=0}^T \tilde{r}_t(s_t, s_{t+1} | \tau_\pi, \tau_E, P) \right], \quad (6)$$

where our original objective (Equation (3)) can be recovered:

$$\max_{\pi} \min_P J(\pi | E, P) = \min_{\pi} \mathbb{E}_{\tau_\pi, \tau_E} [W_1(\tau_\pi, \tau_E)]. \quad (7)$$

As the optimal coupling matrix P can be approximated by the iterative Sinkhorn algorithm [16], the maximization of the objective J with any RL algorithm, can be used as a replacement to minimizing the Wasserstein distance.

Off-policy minimization of the Wasserstein distance. As the reward $\tilde{r}_t(s_t, s_{t+1} | \tau_{\pi_n}, \tau_E, P)$ is defined as a function of a trajectory τ_{π_n} gathered by the learner π_n , any stale reward determined by trajectories from a previous policy π_{n-m} , $m \geq 1$, will not correspond with the Wasserstein distance of the current learner (as noted in Equation (5)). However, working with the assumption that a policy π_n is better than any previous policy with respect to J , (i.e. $J(\pi_n) \geq J(\pi_{n-m})$ where $m \geq 1$), we remark that stale rewards provide an upper bound on the Wasserstein distance:

$$W_1(\tau_{\pi_n}, \tau_E) = \min_P \left(- \sum_{i=0}^T \tilde{r}_t(s_t, s_{t+1} | \tau_{\pi_n}, \tau_E, P) \right) \quad (8)$$

$$\leq \min_P \left(- \sum_{i=0}^T \tilde{r}_t(s_t, s_{t+1} | \tau_{\pi_{n-m}}, \tau_E, P) \right). \quad (9)$$

This means that previously collected off-policy trajectories can be used for learning in a principled manner, at the cost of the tightness of the upper bound of the Wasserstein distance. In our experimental results, we show that reusing prior data dramatically improves the sample efficiency of our algorithm over approaches which rely exclusively on online data [11].

Our final approach, Observational Off-Policy Sinkhorn (OOPS) discovers a reward function in a similar manner to existing approaches [11], [33], but in state transition space rather than state-action space. Unlike these prior approaches, OOPS avoids complexities such as adversarial learning or heuristic-based design of the reward function with multiple hyperparameters. OOPS is summarized in Algorithm 1.

V. EXPERIMENTS

A. Results

We evaluate our algorithm on five MuJoCo locomotion benchmark environments from the OpenAI Gym suite [34], [35], and three robotics tasks [36], [37] in the ILfO setting.

# Expert Traj.		Hopper 3420 \pm 36	Walker2d 4370 \pm 124	HalfCheetah 11340 \pm 95	Ant 5018 \pm 140	Humanoid 5973 \pm 17
1	<i>f</i> -IRL (FKL)	0.91 \pm 0.03	0.42 \pm 0.10	0.63 \pm 0.13	0.47 \pm 0.10	0.47 \pm 0.32
	OPOLO	0.73 \pm 0.09	0.80 \pm 0.14	0.88 \pm 0.02	0.89 \pm 0.04	0.04 \pm 0.01
	SIL - (<i>s</i> , <i>s'</i>)	0.17 \pm 0.06	0.07 \pm 0.02	-0.17 \pm 0.09	-0.41 \pm 0.07	0.07 \pm 0.00
	PWIL - (<i>s</i>)	0.91 \pm 0.14	0.71 \pm 0.30	0.01 \pm 0.01	0.76 \pm 0.05	0.14 \pm 0.14
	OOPS+DDPG (Ours)	0.90 \pm 0.10	0.99 \pm 0.03	1.05 \pm 0.01	1.00 \pm 0.02	0.16 \pm 0.20
	OOPS+TD3 (Ours)	0.98 \pm 0.02	0.95 \pm 0.09	1.05 \pm 0.01	1.00 \pm 0.03	0.74 \pm 0.04
4	<i>f</i> -IRL (FKL)	0.92 \pm 0.04	0.38 \pm 0.12	0.69 \pm 0.12	0.38 \pm 0.07	0.51 \pm 0.28
	OPOLO	0.72 \pm 0.15	0.91 \pm 0.03	0.90 \pm 0.02	1.02 \pm 0.04	0.20 \pm 0.12
	SIL - (<i>s</i> , <i>s'</i>)	0.25 \pm 0.07	0.09 \pm 0.03	-0.22 \pm 0.14	-0.61 \pm 0.22	0.07 \pm 0.01
	PWIL - (<i>s</i>)	0.98 \pm 0.02	0.88 \pm 0.03	0.00 \pm 0.02	0.78 \pm 0.02	0.23 \pm 0.28
	OOPS+DDPG (Ours)	0.75 \pm 0.34	0.96 \pm 0.03	1.05 \pm 0.01	0.99 \pm 0.01	0.07 \pm 0.01
	OOPS+TD3 (Ours)	0.94 \pm 0.07	0.97 \pm 0.01	1.05 \pm 0.01	0.99 \pm 0.03	0.65 \pm 0.15
10	<i>f</i> -IRL (FKL)	0.91 \pm 0.05	0.39 \pm 0.09	0.65 \pm 0.10	0.39 \pm 0.17	0.40 \pm 0.22
	OPOLO	0.66 \pm 0.08	0.96 \pm 0.04	0.95 \pm 0.01	1.00 \pm 0.03	0.16 \pm 0.06
	SIL - (<i>s</i> , <i>s'</i>)	0.17 \pm 0.09	0.08 \pm 0.03	-0.20 \pm 0.09	-0.24 \pm 0.11	0.07 \pm 0.00
	PWIL - (<i>s</i>)	0.98 \pm 0.01	0.87 \pm 0.08	0.01 \pm 0.02	0.78 \pm 0.04	0.23 \pm 0.28
	OOPS+DDPG (Ours)	0.93 \pm 0.03	0.78 \pm 0.39	1.03 \pm 0.04	0.79 \pm 0.38	0.21 \pm 0.25
	OOPS+TD3 (Ours)	0.97 \pm 0.01	0.95 \pm 0.03	1.05 \pm 0.01	1.00 \pm 0.02	0.64 \pm 0.22

TABLE I: Final performance of different ILfO algorithms at 1M timesteps, using 1, 4, 10 expert demonstrations. Values for each task are normalized by the average return of the expert. \pm captures the standard deviation. The highest value and any within 0.05 are **bolded**. The average un-normalized return of the expert is listed below each task. All results are averaged across 5 seeds and 10 evaluations.

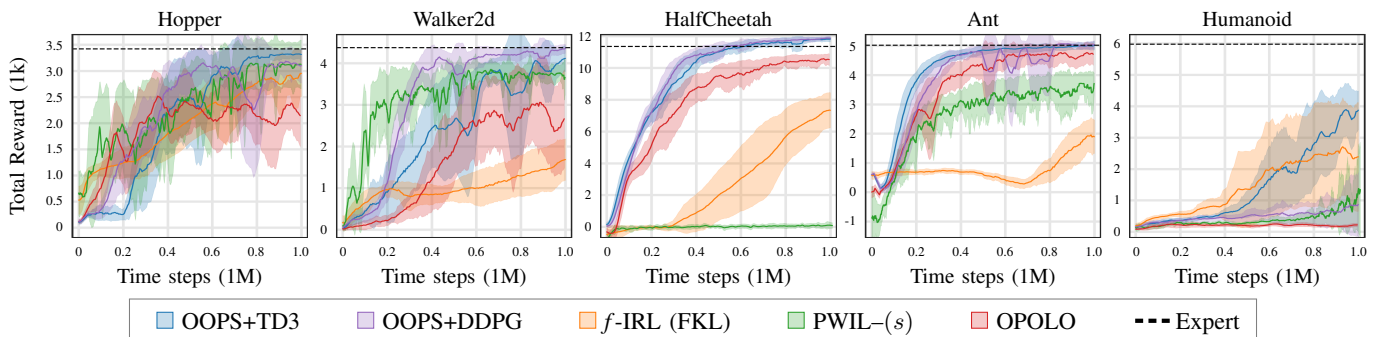


Fig. 1: Learning curves for 1 expert demonstrations across 5 random seeds. The shaded area represents a standard deviation. OOPS+TD3 consistently matches or outperforms the baseline approaches.

For each environment, the dataset of expert trajectories D_E is generated via a pre-trained Soft Actor-Critic agent [38].

We use OOPS to generate a reward function for two RL algorithms, TD3 [39] and DDPG [40]. Our baselines include state of the art ILfO methods: *f*-IRL [7] (its best-performing FKL variant in particular) and OPOLO [13], as well as IL methods which also consider the Wasserstein distance: Primal Wasserstein Imitation Learning (PWIL) [12] and Sinkhorn Imitation Learning (SIL) [11]. In order to compare algorithms in the ILfO setting, we use the state-only version of PWIL, PWIL- (s) [12], and modify SIL [11] by replacing the action a in all pairs (s, a) with the corresponding next state s' in the transition. All algorithms are given a budget of 1M environment interactions (and 1M updates), are evaluated on 5 random seeds, and use the original implementations provided by the authors.

Locomotion. We report the evaluation results of our approach compared against the four baseline algorithms in Table I, varying the number of expert demonstrations used for imitation. The learning curves for the single demonstration setting are shown in Figure 1.

OOPS+TD3 consistently matches, or outperforms, all other baseline methods in every task and for every amount

of expert demonstrations. We also find that OOPS+DDPG can roughly match the performance of the expert in every environment, other than Humanoid. The poor results on Humanoid are unsurprising, as previous results have demonstrated that DDPG tends to fail at the Humanoid task in the standard RL setting [38]. Regardless, since DDPG is known to underperform TD3 and SAC, matching the performance of the SAC expert suggests that the OOPS reward function can produce a stronger learning signal than the original task reward. This shows that OOPS is not dependent on the choice of RL algorithm, assuming the RL algorithm is capable of solving the desired task.

Simulated robotics environments. For the top three performing algorithms (OPOLO, PWIL- (s) , and OOPS+TD3), we also benchmark on three robotics tasks: *BipedalWalker*, a 2D simulated terrain traversal environment, which tests the ability to deal with range sensor data. *Minitaur* is a quadruped locomotion task based on a faithful modeling of Ghost Robotics' Minitaur platform. This PyBullet [36] environment was initially created for Sim-to-Real [37], to transfer learnt running gaits onto a real-world Minitaur. *MinitaurDuck* is a variation of the Minitaur environment that

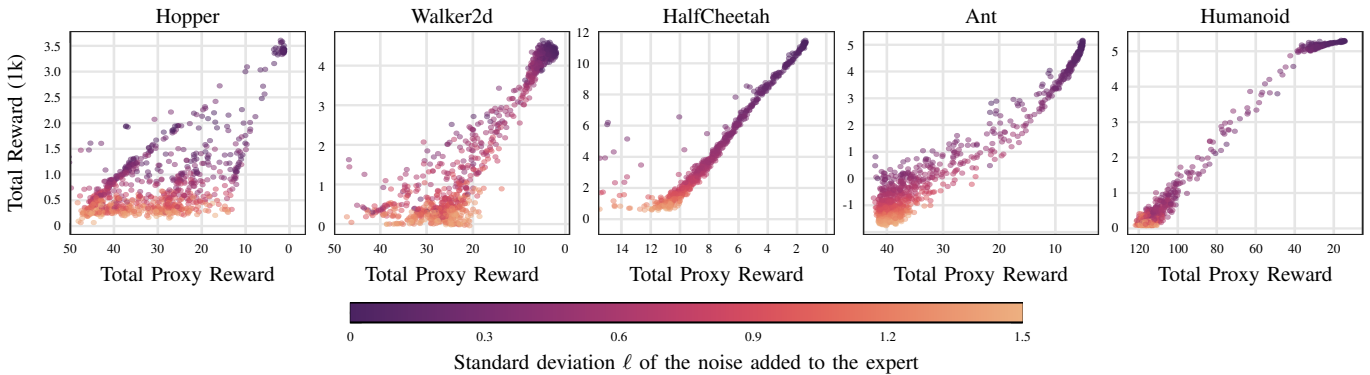


Fig. 2: Calibration plot comparing the proxy reward with the original reward function of the benchmark domains. Each point represents the average of the sum of each reward function, over 5 trajectories. Trajectories are generated by adding noise $\mathcal{N}(0, \ell^2)$ to the expert policy. The calibration plots show a strong correlation between the proxy reward and the true task reward.

# Expert Traj.		BipedalWalker 318.90 \pm 9.20	Minitaur 12.36 \pm 0.75	MinitaurDuck 10.68 \pm 1.20
1	OPOLO	0.96 \pm 0.01	0.76 \pm 0.08	1.00 \pm 0.04
	PWIL - (s)	0.89 \pm 0.01	0.53 \pm 0.19	0.30 \pm 0.14
	OOPS+TD3	0.93 \pm 0.01	1.01 \pm 0.04	0.94 \pm 0.18
4	OPOLO	0.96 \pm 0.01	0.84 \pm 0.09	1.01 \pm 0.03
	PWIL - (s)	0.90 \pm 0.01	0.52 \pm 0.15	0.21 \pm 0.09
	OOPS+TD3	0.92 \pm 0.01	0.91 \pm 0.09	1.02 \pm 0.05
10	OPOLO	0.98 \pm 0.00	0.98 \pm 0.04	1.00 \pm 0.02
	PWIL - (s)	0.88 \pm 0.01	0.58 \pm 0.09	0.15 \pm 0.16
	OOPS+TD3	0.93 \pm 0.01	1.03 \pm 0.03	0.99 \pm 0.09

TABLE II: Final performance of ILfO algorithms on the robotics environments when using 1, 4, and 10 expert demonstrations. Values for each task are normalized by the average return of the expert. \pm captures the standard deviation. The highest value and any within 0.05 are **bolded**. The average un-normalized return of the expert is listed below each task. All results are averaged across 5 seeds and 10 evaluations.

places a duck on top of the Minitaur’s body. The goal is to learn a stable gait without the duck falling off the Minitaur.

We show the results on these robotics environments with varying amounts of expert demonstrations in Table II. While OOPS+TD3 and OPOLO achieve a similar high performance when using all 10 expert demonstrations, OOPS+TD3 surpasses OPOLO when using fewer demonstrations.

B. Analysis and Ablations

To better understand the performance of our approach, in this section, we perform additional analysis to test the quality and importance of various components.

Accuracy of proxy reward. OOPS generates a proxy reward function which minimizes the Wasserstein distance between the learner’s trajectories and the demonstrated expert trajectories. Consequently, if the proxy reward is accurate, it should correlate strongly with the true environment reward. To evaluate this relationship, we collect a dataset of varied trajectory quality using the expert policy from the main results, with added Gaussian noise $\mathcal{N}(0, \ell^2)$ with $\ell \in [0, 1.5]$. Figure 2 shows the calibration plots between the proxy reward and the original task reward, showing a strong correlation in every environment.

Next we compare the quality of trajectories, in terms

of the Wasserstein distance, rather than the true environment reward. In Table III, we compare the Wasserstein distance between the expert trajectories and the final policy rollouts obtained at the end of training from each of the top-3 performing methods (OOPS, OPOLO, PWIL- (s)). The Wasserstein distance is measured in three spaces: state-only (s), state-transition (s, s'), and state-action (s, a).

We find that OOPS obtains the lowest state-action Wasserstein distance to the expert trajectories in four of the five studied environments, with Walker2d being the only disagreement with the previous experiment, as even though OOPS+TD3 obtains a better task reward in Table I, PWIL- (s) obtains a lower state-action Wasserstein distance to the expert. To further evaluate the quality of the Wasserstein distance used by PWIL, we take OOPS and replace the Sinkhorn algorithm with the greedy formulation W_{greedy} proposed by PWIL to compute the Wasserstein distance in (s, s') space. The results are reported in Table IV (under W_{greedy}), and show a loss in performance.

Quality of estimated Wasserstein distance. We now evaluate the quality of our estimated Wasserstein distance.

In Figure 3, we compare the quality of different approximations of the state transition Wasserstein distance: the Sinkhorn distance W_{sk} with varying λ , the network simplex solver $W_{simplex}$ introduced in [41], and W_{greedy} proposed for PWIL [12]. To compare each approach, we compute the Wasserstein distance between trajectories generated by the final policy of OOPS+TD3 and the expert trajectories, using each of the various approximations. As each method results in different estimates of the coupling matrix P , they all provide an upper bound on the true Wasserstein distance, where lower estimates of Wasserstein distance is a tighter bound. We find that for very low values of λ , W_{sk} computes lower cost couplings than $W_{simplex}$, and up to $\lambda \approx 0.4$ obtains better approximations than W_{greedy} .

Next, we compare these three approaches for computing the Wasserstein distance in terms of performance. The results are shown in Table IV (Wasserstein Distance Solver). Unsurprisingly, large values of λ , which approximate the Wasserstein distance W_1 poorly, results in lower performance. For sufficiently small values of λ , we find that OOPS+TD3

Environment Space	Hopper			Walker2d			HalfCheetah			Ant			Humanoid		
	(s)	(s, s')	(s, a)	(s)	(s, s')	(s, a)	(s)	(s, s')	(s, a)	(s)	(s, s')	(s, a)	(s)	(s, s')	(s, a)
OPOLO	5.91	8.40	6.33	3.02	4.32	3.47	1.60	2.39	1.91	4.64	7.24	5.05	80.75	114.53	81.90
PWIL – (s)	1.74	2.56	2.38	2.04	2.96	2.78	6.48	9.27	6.93	3.83	6.00	5.90	53.52	76.06	54.94
OOPS+TD3	1.66	2.38	2.06	2.28	3.27	3.02	1.63	2.41	2.01	3.83	5.90	5.17	25.64	37.03	27.63

TABLE III: Final Wasserstein distance in state occupancy, state transition, and state-action space of the 10 final trained agent rollouts to the expert trajectories for different ILfO algorithms, lower is better. We highlight in **blue** the best performing agent in state-action space, considered ground truth in this experiment, and **bold** the best performing agent according to each metric. Agents were trained using 10 expert demonstration trajectories, for 1M timesteps. Distances are averaged over 10 reference expert trajectories.

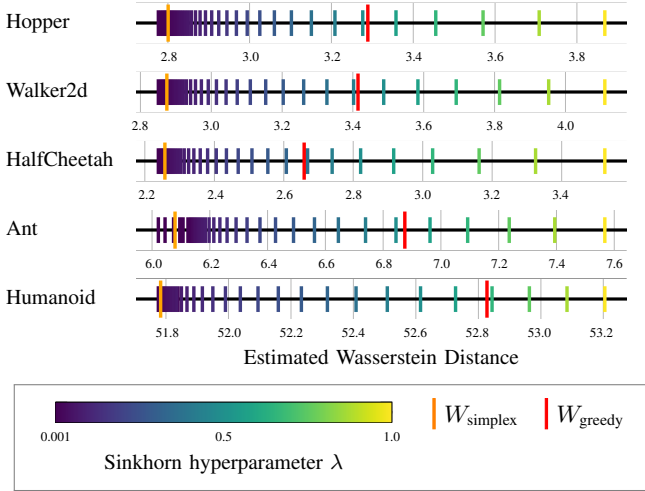


Fig. 3: Wasserstein distances between the 10 final rollout trajectories of OOPS+TD3 and the expert, using different solvers for the coupling matrix P (W_{greedy} and W_{simplex}) compared against the Sinkhorn distance W_{sk} when varying the parameter λ . Results are averaged over 10 expert trajectories. The Sinkhorn distance, for low enough values of λ computes a tighter upper bound to the Wasserstein distance estimates than W_{greedy} [12].

maintains a consistent performance. This suggests that λ can generally be ignored and left to a default value.

Finally, we attempt different settings for the Wasserstein distance. In Table IV we display the change in performance from OOPS when using W_1 or W_2 when the distance metric d is the Euclidean distance $\|\cdot\|_2$, and W_1 when d is the cosine distance. OOPS uses W_1 with the square root of the Euclidean distance, which de-emphasizes large differences in magnitude in a similar fashion to the cosine distance. We find that this choice of d provides significant benefits in high dimensional domains (Humanoid) where magnitudes matter but can vary significantly. We also compare with the learnt adversarial distance metric used by SIL [11] (denoted OOPS_{adv}), and find that while this version outperforms vanilla SIL, the adversarial component is harmful.

Transition vs. state occupancy. For OOPS, we define trajectories by their state-next-state transitions (s, s') , rather than individual states s . Matching based on states can potentially admits multiple minimums since trajectories with the same states out of order can still minimize the state occupation distributional distance. Furthermore, if the reward function is based on state *and* action, then it is clear that only matching state occupancy is insufficient. This setting is far more common in robotics as the reward is often defined by change, such as an increase in velocity, and

	Hopper	Walker2d	HalfCheetah	Ant	Humanoid
Occupancy (Default: (s, s'))					
State only	0.10	-33.93	-0.57	0.30	-0.94
Wasserstein Distance Solver (Default: $\lambda = 0.05$)					
W_{greedy}	-14.99	-7.75	-45.46	-0.79	-19.21
W_{simplex}	-10.91	-6.09	-1.03	-2.40	-33.99
$\lambda = 0.005$	-3.12	-2.65	-0.35	-1.48	-2.34
$\lambda = 0.1$	-1.72	-3.87	-1.39	-3.88	-9.18
$\lambda = 0.5$	-58.64	-25.20	-15.09	-10.95	-24.44
Wasserstein Distance Variations (Default: $W_1, d = \sqrt{\ \cdot\ _2}$)					
$W_2, d = \ \cdot\ _2$	-36.52	-21.83	-11.88	-16.10	-47.92
$W_1, d = \ \cdot\ _2$	-4.61	-1.42	-1.73	-1.95	-22.80
$W_1, d = \cos$	0.13	-10.04	-4.09	-2.84	-34.63
Adversarial Distance (Default: Unused)					
SIL – (s, s')	-82.50	-91.61	-119.10	-124.88	-90.83
OOPS_{adv}	-21.09	-76.58	-101.84	-17.68	-97.87

TABLE IV: Results different variations of OOPS in terms of percent difference. All results use 10 expert trajectories, and are averaged across 5 seeds and 10 evaluations. State only uses W_1 over (s) rather than (s, s') . Wasserstein distance solver modifies the solver used by OOPS to determine the coupling matrix P . Adversarial distance refers to the use of the adversarial distance function from SIL [11] and also includes the full SIL method for comparison.

typically considers costs associated with the action space. Since expert actions are unavailable in the ILfO setting, we must rely on (s, s') , which offers a strong approximation as the outcome s' is defined as a function of both the state s and action a . We posit that enforcing a local ordering of states provides a higher fidelity signal for ILfO. We validate this empirically in our ablations (Table IV). While using state-only occupancy matches the performance of OOPS+TD3 in most environments, there is a large drop in performance in Walker2d. This aligns with our intuition: matching by state occupancy will typically provide a good matching, but can be problematic in certain environments depending on the state representation and transition dynamics.

VI. CONCLUSION

In this paper, we introduce OOPS, an ILfO algorithm that produces a reward function which minimizes the Wasserstein distance between the state transition trajectory of the expert and the imitation agent. We validate our approach through an extensive set of experiments and demonstrate that OOPS surpasses the current state-of-the-art methods in the ILfO setting across benchmark and robotics domains. Combined with off-policy RL, OOPS exhibits exceptional sample efficiency and low variance in performance, key qualities for the practical deployment of IL algorithms on real systems.

REFERENCES

- [1] T. Haarnoja, A. Zhou, K. Hartikainen, G. Tucker, S. Ha, J. Tan, V. Kumar, H. Zhu, A. Gupta, P. Abbeel, *et al.*, “Soft actor-critic algorithms and applications,” *arXiv preprint arXiv:1812.05905*, 2018.
- [2] D. Kalashnikov, A. Irpan, P. Pastor, J. Ibarz, A. Herzog, E. Jang, D. Quillen, E. Holly, M. Kalakrishnan, V. Vanhoucke, *et al.*, “Scalable deep reinforcement learning for vision-based robotic manipulation,” in *Conference on Robot Learning*, 2018, pp. 651–673.
- [3] S. Desai, I. Durugkar, H. Karnan, G. Warnell, J. Hanna, P. Stone, and A. Sony, “An imitation from observation approach to sim-to-real transfer,” 2020.
- [4] R. Kidambi, J. Chang, and W. Sun, “Mobile: Model-based imitation learning from observation alone,” *Advances in Neural Information Processing Systems*, vol. 34, 2021.
- [5] J. Ho and S. Ermon, “Generative adversarial imitation learning,” in *Advances in Neural Information Processing Systems*, 2016, pp. 4565–4573.
- [6] S. K. S. Ghasemipour, R. Zemel, and S. Gu, “A divergence minimization perspective on imitation learning methods,” in *Conference on Robot Learning*. PMLR, 2020, pp. 1259–1277.
- [7] T. Ni, H. Sikchi, Y. Wang, T. Gupta, L. Lee, and B. Eysenbach, “f-irl: Inverse reinforcement learning via state marginal matching,” in *Conference on Robot Learning*, 2020.
- [8] M. Cuturi, “Sinkhorn distances: Lightspeed computation of optimal transport,” *Advances in neural information processing systems*, vol. 26, 2013.
- [9] N. Bonneel, J. Rabin, G. Peyré, and H. Pfister, “Sliced and radon wasserstein barycenters of measures,” *Journal of Mathematical Imaging and Vision*, vol. 51, no. 1, pp. 22–45, 2015.
- [10] I. Kostrikov, K. K. Agrawal, D. Dwibedi, S. Levine, and J. Tompson, “Discriminator-actor-critic: Addressing sample inefficiency and reward bias in adversarial imitation learning,” in *7th International Conference on Learning Representations, ICLR 2019, New Orleans, LA, USA, May 6-9, 2019*. OpenReview.net, 2019. [Online]. Available: <https://openreview.net/forum?id=Hk4fpoA5Km>
- [11] G. Papagiannis and Y. Li, “Imitation learning with sinkhorn distances,” *arXiv preprint arXiv:2008.09167*, 2020.
- [12] R. Dadashi, L. Hussenot, M. Geist, and O. Pietquin, “Primal wasserstein imitation learning,” in *International Conference on Learning Representations*, 2020.
- [13] Z. Zhu, K. Lin, B. Dai, and J. Zhou, “Off-policy imitation learning from observations,” *Advances in Neural Information Processing Systems*, vol. 33, pp. 12402–12413, 2020.
- [14] C. Villani, *Optimal transport: old and new*. Springer, 2009, vol. 338.
- [15] G. Peyré, M. Cuturi, *et al.*, “Computational optimal transport: With applications to data science,” *Foundations and Trends® in Machine Learning*, vol. 11, no. 5-6, pp. 355–607, 2019.
- [16] R. Sinkhorn, “Diagonal equivalence to matrices with prescribed row and column sums,” *The American Mathematical Monthly*, vol. 74, no. 4, pp. 402–405, 1967.
- [17] B. D. Ziebart, A. L. Maas, J. A. Bagnell, and A. K. Dey, “Maximum entropy inverse reinforcement learning,” in *AAAI*, vol. 8, 2008, pp. 1433–1438.
- [18] J. Fu, K. Luo, and S. Levine, “Learning robust rewards with adversarial inverse reinforcement learning,” *arXiv preprint arXiv:1710.11248*, 2017.
- [19] I. Kostrikov, K. K. Agrawal, D. Dwibedi, S. Levine, and J. Tompson, “Discriminator-actor-critic: Addressing sample inefficiency and reward bias in adversarial imitation learning,” in *International Conference on Learning Representations*, 2018.
- [20] L. Ke, M. Barnes, W. Sun, G. Lee, S. Choudhury, and S. Srinivasa, “Imitation learning as f -divergence minimization,” *arXiv preprint arXiv:1905.12888*, 2019.
- [21] F. Torabi, G. Warnell, and P. Stone, “Behavioral cloning from observation,” in *Proceedings of the 27th International Joint Conference on Artificial Intelligence*, 2018, pp. 4950–4957.
- [22] A. Jaegle, Y. Sulsky, A. Ahuja, J. Bruce, R. Fergus, and G. Wayne, “Imitation by predicting observations,” in *International Conference on Machine Learning*. PMLR, 2021, pp. 4665–4676.
- [23] W.-D. Chang, J. C. G. Higuera, S. Fujimoto, D. Meger, and G. Dudek, “Il-flow: Imitation learning from observation using normalizing flows,” *arXiv preprint arXiv:2205.09251*, 2022.
- [24] W. Sun, A. Vemula, B. Boots, and D. Bagnell, “Provably efficient imitation learning from observation alone,” in *International Conference on Machine Learning*. PMLR, 2019, pp. 6036–6045.
- [25] F. Torabi, G. Warnell, and P. Stone, “Generative adversarial imitation from observation,” *arXiv preprint arXiv:1807.06158*, 2018.
- [26] H. Xiao, M. Herman, J. Wagner, S. Ziesche, J. Etesami, and T. H. Linh, “Wasserstein adversarial imitation learning,” *arXiv preprint arXiv:1906.08113*, 2019.
- [27] M. Zhang, Y. Wang, X. Ma, L. Xia, J. Yang, Z. Li, and X. Li, “Wasserstein distance guided adversarial imitation learning with reward shape exploration,” in *2020 IEEE 9th Data Driven Control and Learning Systems Conference (DDCLS)*, Nov 2020, pp. 1165–1170.
- [28] M. Arjovsky, S. Chintala, and L. Bottou, “Wasserstein generative adversarial networks,” in *International conference on machine learning*. PMLR, 2017, pp. 214–223.
- [29] M. Arjovsky and L. Bottou, “Towards principled methods for training generative adversarial networks,” in *International Conference on Learning Representations*, 2017. [Online]. Available: https://openreview.net/forum?id=Hk4_qw5xe
- [30] J. Stanczuk, C. Etmann, L. M. Kreusser, and C.-B. Schönlieb, “Wasserstein gans work because they fail (to approximate the wasserstein distance),” *arXiv preprint arXiv:2103.01678*, 2021.
- [31] S. Haldar, V. Mathur, D. Yarats, and L. Pinto, “Watch and match: Supercharging imitation with regularized optimal transport,” in *Conference on Robot Learning*. PMLR, 2023, pp. 32–43.
- [32] J. Schulman, S. Levine, P. Abbeel, M. Jordan, and P. Moritz, “Trust region policy optimization,” in *International Conference on Machine Learning*, 2015, pp. 1889–1897.
- [33] R. Dadashi, L. Hussenot, M. Geist, and O. Pietquin, “Primal wasserstein imitation learning,” *arXiv preprint arXiv:2006.04678*, 2020.
- [34] E. Todorov, T. Erez, and Y. Tassa, “Mujoco: A physics engine for model-based control,” in *IEEE/RSJ International Conference on Intelligent Robots and Systems (IROS)*. IEEE, 2012, pp. 5026–5033.
- [35] G. Brockman, V. Cheung, L. Pettersson, J. Schneider, J. Schulman, J. Tang, and W. Zaremba, “Openai gym,” 2016.
- [36] E. Coumans and Y. Bai, “Pybullet, a python module for physics simulation for games, robotics and machine learning,” 2016.
- [37] J. Tan, T. Zhang, E. Coumans, A. Iscen, Y. Bai, D. Hafner, S. Bohez, and V. Vanhoucke, “Sim-to-real: Learning agile locomotion for quadruped robots,” in *Proceedings of Robotics: Science and Systems*, Pittsburgh, Pennsylvania, June 2018.
- [38] T. Haarnoja, A. Zhou, P. Abbeel, and S. Levine, “Soft actor-critic: Off-policy maximum entropy deep reinforcement learning with a stochastic actor,” in *International Conference on Machine Learning*, vol. 80. PMLR, 2018, pp. 1861–1870.
- [39] S. Fujimoto, H. van Hoof, and D. Meger, “Addressing function approximation error in actor-critic methods,” in *International Conference on Machine Learning*, vol. 80. PMLR, 2018, pp. 1587–1596.
- [40] T. P. Lillicrap, J. J. Hunt, A. Pritzel, N. Heess, T. Erez, Y. Tassa, D. Silver, and D. Wierstra, “Continuous control with deep reinforcement learning,” *arXiv preprint arXiv:1509.02971*, 2015.
- [41] N. Bonneel, M. van de Panne, S. Paris, and W. Heidrich, “Displacement interpolation using lagrangian mass transport,” *ACM Trans. Graph.*, vol. 30, no. 6, p. 1–12, dec 2011. [Online]. Available: <https://doi.org/10.1145/2070781.2024192>